Binding of 1-Benzopyran-4-one Derivatives to Aldose Reductase: A Free Energy Perturbation Study

ARTICLE *in* BIOORGANIC & MEDICINAL CHEMISTRY · JUNE 2002

Impact Factor: 2.79 · DOI: 10.1016/S0968-0896(01)00408-4 · Source: PubMed

8 AUTHORS, INCLUDING:

Maria Cristina Gamberini
Università degli Studi di Modena e Reggio E...
31 PUBLICATIONS **642** CITATIONS
SEE PROFILE

Antonella Del Corso
Università di Pisa
80 PUBLICATIONS **1,371** CITATIONS
SEE PROFILE

Umberto Mura
Università di Pisa
104 PUBLICATIONS **1,475** CITATIONS
SEE PROFILE

AM Ferrari
.
10 PUBLICATIONS **419** CITATIONS
SEE PROFILE

Pergamon

Bioorganic & Medicinal Chemistry 10 (2002) 1427–1436

BIOORGANIC & MEDICINAL CHEMISTRY

Binding of 1-Benzopyran-4-one Derivatives to Aldose Reductase: A Free Energy Perturbation Study

Giulio Rastelli,[a,*] Luca Costantino,[a] M. Cristina Gamberini,[a] Antonella Del Corso,[b] Umberto Mura,[b] J. Mark Petrash,[c] Anna Maria Ferrari[a] and Sara Pacchioni[a]

[a]*Dipartimento di Scienze Farmaceutiche, Universita di Modena e Reggio Emilia, Via Campi, 183, 41100 Modena, Italy*
[b]*Dipartimento di Fisiologia e Biochimica, Università di Pisa, Via S. Maria, 55, 56100 Pisa, Italy*
[c]*Department of Ophthalmology and Visual Sciences, Washington University, School of Medicine, St. Louis, MI 63110, USA*

Received 25 September 2001; accepted 16 November 2001

Abstract—The relative binding affinities to human aldose reductase (ALR2) of three new 7-hydroxy-2-benzyl-4*H*-1-benzopyran-4-one inhibitors were predicted by free energy perturbation (FEP) simulations. Molecular substitutions were specifically designed to investigate the role of hydrogen bonding at the active site of ALR2. Starting from the lead inhibitor 7-hydroxy-2-(4′-hydroxybenzyl)-4*H*-1-benzopyran-4-one, the 4′-hydroxyl was mutated to methyl and to trifluoromethyl, and an hydroxyl at position 8 was additionally introduced. Once synthesized and tested as inhibitors of ALR2, the compounds displayed variations of K_i that were in qualitative to quantitative agreement with the calculated relative free energies of binding. The results, discussed in terms of balance between free energies of solvation and free energies of binding to ALR2, elucidate the importance of hydrogen bonding with Thr113 and with Trp111 and cofactor, and provide a rationale to the observed differences in binding affinities.

Introduction

Aldose reductase (ALR2; EC1.1.1.21) is an important enzyme in the development of degenerative complications of diabetes mellitus, through its ability to reduce excess D-glucose into D-sorbitol with the associated conversion of NADPH to $NADP^+$.[1] Available experimental data link D-glucose metabolism to long-term diabetic complications such as cataract, neuropathy, nephropathy, and retinopathy. Aldose reductase inhibitors should therefore be able to safely prevent or arrest the development of diabetic complications.[1]

To date, two main classes of ALR2 inhibitors have been reported, namely carboxylic acids and spirohydantoins.[2,3] However, carboxylic acids possess in vivo activity lower than spirohydantoins, probably because their acidic nature results in poor pharmacokinetics. On the other hand, spirohydantoins like Sorbinil, which are less acidic than carboxylic acids and posses better pharmacokinetic properties, cause hypersensitivity reactions.[2,4] Therefore, new ALR2 inhibitors not structurally related to carboxylic acids and spyrohydantoins, and possibly having pK_a values higher than carboxylic acids, are highly desirable.

In a recent publication, we reported that 1-benzopyran-4-one derivatives are potent and selective inhibitors of ALR2.[5] The combination of ALR2 activity and selectivity with respect to the closely related enzyme aldehyde reductase (ALR1) appears promising for the development of drugs effective against diabetic complications.[5] As an additional advantage, 1-benzopyran-4-one derivatives are considerably less acidic than carboxylic acids: the 7-hydroxyl group of 1-benzopyran-4-one, which turned out to be one of the most important structural requirements for ALR2 inhibition,[5] has a pK_a of 7.3.[6]

In the crystal structures of the complexes between ALR2 and Zopolrestat[7] or Tolrestat[8] as well as in previous molecular modeling studies,[9–12] the carboxylic acid derivatives bind ALR2 with the carboxylate interacting with Tyr48 and His110, which are two key residues in binding and catalysis.[13,14] Docking of 7-hydroxy-benzopyran-4-one derivatives into the ALR2

*Corresponding author. Tel.: +39-059-205-5145; fax +39-059-205-5131; e-mail: rastelli.giulio@unimo.it

0968-0896/02/$ - see front matter
PII: S0968-0896(01)00408-4

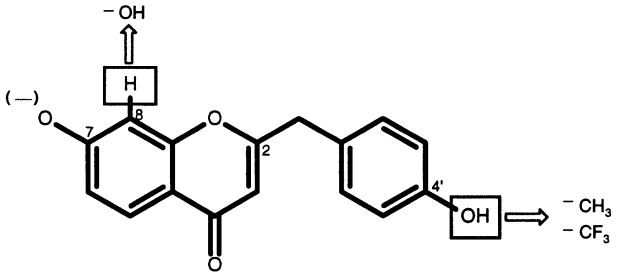

Scheme 1. Substituents explored with free energy perturbation.

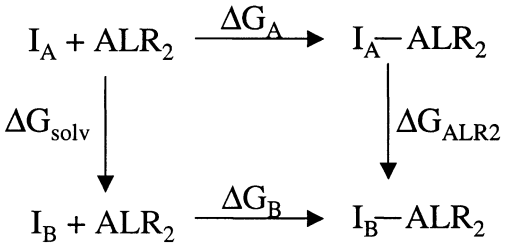

Scheme 2. Free energy perturbation cycle.

structure and molecular mechanics calculations of the complexes predicted that the dissociated 7-hydroxyl hydrogen bonds to Tyr48 and His110, thus resembling the carboxylate function of previously known inhibitors.[5] In Figure. 1, a selection of aminoacidic residues interacting with one of the most active inhibitors of this class [7-hydroxy-2-(4′-hydroxybenzyl)-4*H*-1-benzopyran-4-one][5] is presented. In addition to the hydrogen bonds established between the dissociated 7-hydroxyl and Tyr48 and His110, the 4′-hydroxyl hydrogen bonds to Thr113. The 2-(4′-hydroxylbenzyl) substituent, in fact, is able to bind the so-called 'specificity pocket', in line with previous crystallographic[7,8] and modeling[9–12] studies of ALR2–inhibitor complexes. These studies showed that conformational changes upon binding of suitable hydrophobic-aromatic inhibitors lead to the opening of this additional pocket, which is lined by Trp111 and Leu300, and that inhibitors that bind this pocket are selective for ALR2 with respect to ALR1, as indeed is the case of the 7-hydroxy-2-benzyl-4*H*-1-benzopyran-4-one derivatives previously reported.[5]

In the present work, we predict the effects of structural modifications of the inhibitor 7-hydroxy-2-(4′-hydroxybenzyl)-4*H*-1-benzopyran-4-one using free energy perturbation[15] (FEP) calculations. In many cases, predictions based on this methodology led to free energy differences of binding that were in qualitative to quantitative agreement with experiment.[16–18] Moreover, when applied systematically to a series of protein–inhibitor complexes, FEP predictions were found to closely match the inhibitory activity trend observed experimentally.[19]

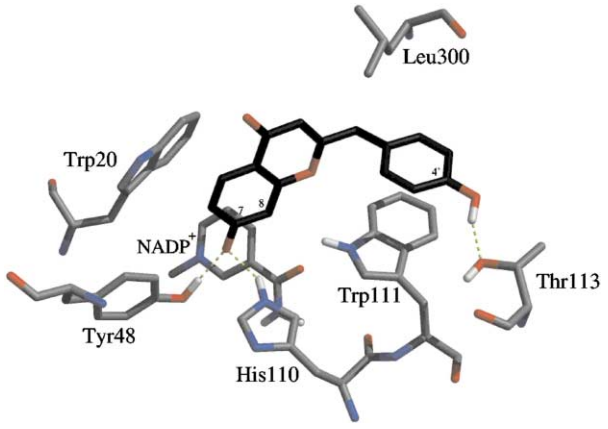

Figure 1. Residues of the active site of ALR2 that interact with the reference inhibitor 7-hydroxy-2-(4′-hydroxybenzyl)-4*H*-1-benzopyran-4-one.

Here, two substitution sites were chosen for modification (Scheme 1). In the structure of the complex, the 4′OH acts as a hydrogen bond donor to the hydroxyl of Thr113 (Fig. 1). To investigate the importance of the 4′-hydroxyl as a hydrogen bond donor to Thr113, the hydroxyl was mutated to methyl (hydrophobic) and to trifluoromethyl (hydrophobic and weak hydrogen bond acceptor) (Scheme 1). Secondly, an additional hydroxyl group at position 8 was introduced because it could provide two additional hydrogen bonds, one with the amino hydrogen of Trp111 and one with the carbonyl oxygen of the nicotinamide of $NADP^+$ (Fig. 1). Removal of the 4′-hydroxyl by mutation to hydrophobic substituents reduces desolvation energy and should facilitate binding. In contrast, introduction of a hydroxyl group at the 8 position provides stronger interactions with ALR2 which should compensate for the higher desolvation cost.

To compare the predicted and the experimental free energies of binding, the derivatives reported in Scheme 1 were synthesized and tested as inhibitors of human ALR2.

Results

The FEP methodology was applied to calculate both solvation free energy differences in water and binding free energy differences to ALR2 between the analogues reported in Scheme 1. We used the thermodynamic perturbation method[20–22] to calculate the free energy differences.

The thermodynamic cycle relevant to this study is shown in Scheme 2. The free energies of binding to the protein of the two related inhibitors I_A and I_B, ΔG_A and ΔG_B, are difficult to calculate and are determined experimentally. ΔG_{solv} corresponds to mutating I_A into I_B in water, while ΔG_{ALR2} corresponds to mutating I_A into I_B while bound to ALR2 in water. Since the thermodynamic cycle is closed and free energy is a state function, the relative binding free energy is $\Delta\Delta G_{bind} = \Delta G_B - \Delta G_A = \Delta G_{ALR2} - \Delta G_{solv}$. While ΔG_{solv} and ΔG_{ALR2} represent physically unrealizable processes, these two simulations are computationally manageable.

In the present work, the reference inhibitor (I_A) was 7-hydroxy-2-(4′-hydroxybenzyl)-4*H*-1-benzopyran-4-one

Table 1. Calculated relative solvation and binding free energies (kcal/mol) between 7-hydroxy-2-(4′-hydroxybenzyl)-4*H*-1-benzopyran-4-one (4′OH) and its analogues

Mutation	Run	Length (ps)	ΔG_{solv}	$<\Delta G>_{solv}$	ΔG_{ALR2}	$<\Delta G>_{ALR2}$
4′OH→4′CH_3	Forward	160	5.57±0.06	5.64±0.07	5.34±0.07	5.49±0.15
	Reverse		−5.71±0.02		−5.63±0.14	
	Forward	400	5.73±0.04	5.79±0.06	5.99±0.10	6.21±0.21
	Reverse		−5.84±0.03		−6.42±0.07	
	Forward	600	5.70±0.03	5.72±0.02	6.43±0.20	6.29±0.14
	Reverse		−5.74±0.02		−6.15±0.18	
4′OH→4′CF_3	Forward	160	10.40±0.51	10.10±0.30	10.16±0.33	10.13±0.04
	Reverse		−9.80±0.11		−10.09±0.20	
	Forward	400	9.99±0.11	10.09±0.10	11.95±0.04	11.64±0.31
	Reverse		−10.19±0.16		−11.33±0.15	
	Forward	600	9.87±0.25	10.09±0.22	11.96±0.02	11.58±0.39
	Reverse		−10.31±0.29		−11.19±0.27	
8H→8OH	Forward	160	−1.83±0.01	−1.90±0.07	−0.60±0.01	−0.59±0.02
	Reverse		1.97±0.08		0.57±0.04	
	Forward	400	−2.46±0.08	−2.64±0.18	−0.29±0.02	−0.41±0.11
	Reverse		2.83±0.22		0.52±0.01	
	Forward	600	−2.16±0.07	−2.43±0.27	−0.53±0.01	−0.65±0.12
	Reverse		2.69±0.29		−0.76±0.04	

(4′OH), and the starting I_A–ALR2 structure was taken from our previous work.[5] The free energy changes upon mutating the inhibitors are given in Table 1. Both forward and reverse simulations were performed, and the resulting ΔG values were averaged. Simulations of different lengths, ranging from 160 to 600 ps, were done to check convergence of the free energy results. To compare with experimental results, the new derivatives were synthesized, and their experimental inhibition constants (K_i) of human ALR2 were determined. The K_i values, the values of ΔG_A and ΔG_B inferred from the K_i's, and the experimental ($\Delta\Delta G_{expt}$) and calculated ($\Delta\Delta G_{bind}$) free energy differences of binding are reported in Table 2.

Table 2. Inhibition constants (K_i) against human aldose reductase, and comparison of experimental ($\Delta\Delta G_{expt}$) and calculated ($\Delta\Delta G_{bind}$) free energy differences of binding relative to 4′OH

	K_i ^{hALR2} (μM)	ΔG_{expt}[a]	$\Delta\Delta G_{expt}$[b]	$\Delta\Delta G_{bind}$[c]
4′OH	0.18±0.08	−9.26±0.28		
4′CH_3	1.17±0.08	−8.14±0.08	1.12±0.29	0.57±0.14
4′CF_3	2.95±0.01	−7.59±0.01	1.67±0.28	1.49±0.45
8OH	10.4±0.68	−6.84±0.08	2.42±0.29	1.78±0.30

[a]Experimental free energies of binding calculated from the equation $\Delta G = -RT\ln 1/K_i$, and expressed in kcal/mol.
[b]Experimental free energy differences of binding relative to the reference compound 4′OH.
[c]Calculated free energies of binding relative to 4′OH, expressed as the difference between $<\Delta G>_{ALR2}$ and $<\Delta G>_{solv}$ of the longer (600 ps) simulations of Table 1.

Solvation free energies

The solvation free energies of 4′CH_3 relative to 4′OH are 5.64±0.07, 5.79±0.06 and 5.72±0.02 kcal/mol for the 160, 400 and 600 ps simulations, respectively (Table 1). The free energies of relative solvation calculated in the forward (4′OH→4′CH_3) and reverse (4′CH_3→4′OH) directions are fairly similar, giving very low hysteresys. The positive sign of ΔG_{solv} indicates that the 4′CH_3 derivative is less solvated than the reference 4′OH derivative, in agreement with a polar hydroxyl being mutated to a methyl.

The predicted changes in solvation free energy of 4′CF_3 relative to 4′OH are 10.10±0.30, 10.09±0.10 and 10.09±0.22 kcal/mol for the 160, 400 and 600ps simulations, respectively (Table 1). Compared with the 4′OH→4′CH_3 perturbation, the 4′OH→4′CF_3 mutation gives remarkably higher values of ΔG_{solv}. This difference is estimated to be about 4.4 kcal/mol. Therefore, the trifluoromethyl substituent turns out to be significantly more hydrophobic than the methyl substituent of our lead inhibitors. Actually, whether fluorine and fluoroalkyl substituents can or cannot act as hydrogen bond acceptors is a matter of debate.[23,24] If they can, the trifluoromethyl substituent would be expected to be more solvated than the methyl, in contrast with the present results. Even though the AMBER force-field parameterized by Cornell et al.[25] does not contain an explicit hydrogen bonding term, hydrogen bonds in proteins, nucleic acids and organic molecules in such a 'minimalist' force-field are consistently described by the electrostatic and van der Waals terms.[25–29] In this respect, the ability of fluorine to act as a potential hydrogen bond acceptor is, indeed, guaranteed by the fact that fluorine is negatively charged in our inhibitors (Scheme 3) as well as in the CF4 and CHCF3 molecules used to derive the fluorine parameters for AMBER.[30] Therefore, interaction with a hydrogen bond donor would lead, in principle, to a favourable electrostatic interaction energy. With this in mind, the finding that the trifluoromethyl substituent is significantly more hydrophobic than the methyl substituent can likely be attributed to effects other than electrostatics, such as van der Waals effects. Indeed, only rarely is fluorine seen to act as a hydrogen bond acceptor,[23] and water–octanol partition coefficients indicate that the trifluoromethyl substituent is more hydrophobic than the

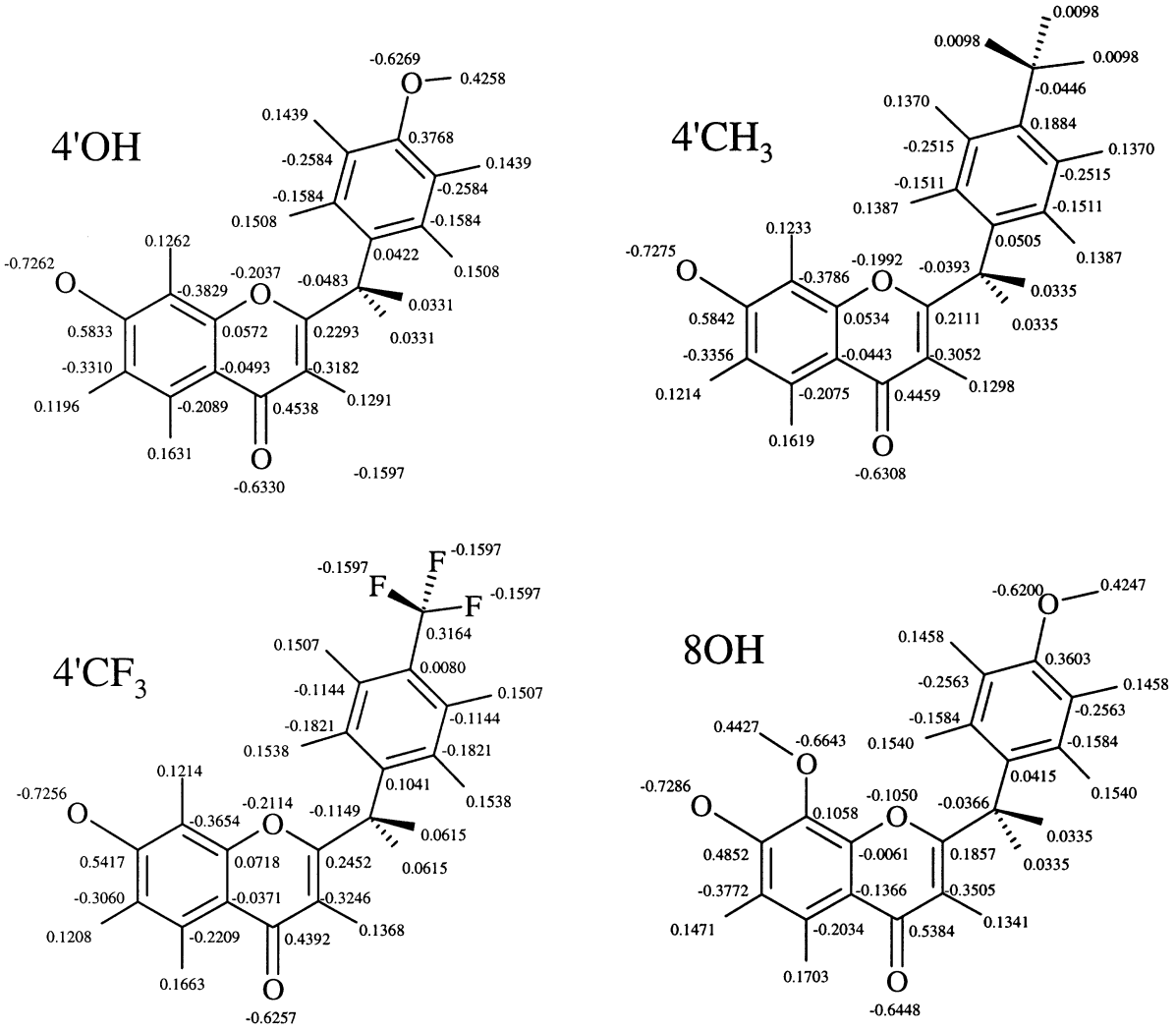

Scheme 3. Partial charges of the 4′OH, 4′CH3, 4′CF3 and 8OH inhibitors.

methyl (π constants being 0.88 for trifluoromethyl and 0.56 for methyl), in line with the free energy differences of solvation found here.

Finally, an additional hydroxyl group was introduced at position 8 (8H→8OH). As expected, the 8OH derivative is more solvated than the reference compound. The changes in free energy of solvation are -1.90 ± 0.07, -2.64 ± 0.18 and -2.43 ± 0.27 kcal/mol for the 160, 400 and 600ps simulations, respectively (Table 1).

ALR2 binding free energies

The free energy differences obtained from the mutations into the solvated binding site of aldose reductase (ΔG_{ALR2}) are also given in Table 1.

The predicted free energy changes upon mutating 4′OH into 4′CH_3 (4′OH→4′CH_3) in ALR2 are 5.49 ± 0.15, 6.21 ± 0.21 and 6.29 ± 0.14 kcal/mol for the 160, 400 and 600 ps simulations, respectively (Table 1). According to the positive sign of these free energies, the 4′CH_3 derivative is predicted to form an ALR2–inhibitor complex which is less stable than that of the reference inhibitor 4′OH. Indeed, the 4′CH_3 derivative costs 5.72 kcal/mol less to desolvate but looses 6.29 kcal/mol in the complex with ALR2 as compared to 4′OH, resulting in a $\Delta\Delta G_{bind}$ of 0.57 kcal/mol (Table 2). Therefore, the 4′CH_3 derivative is predicted to bind less effectively to ALR2. The orientation of 4′CH3 into the ALR2 binding site is depicted in Fig. 2 (a), where the structure has been overlayed with that of 4′OH for comparison. While both inhibitors form hydrogen bonds with Tyr48 and His110, only 4′OH hydrogen bonds to Thr113. As a result of unfavorable interactions between the 4′-methyl and the Thr113 hydroxyl, the inhibitor and the Thr113 residue are both displaced compared to 4′OH [Fig. 2(a)].

The free energy differences obtained after mutating 4′OH into 4′CF_3 in ALR2 are 10.13 ± 0.04, 11.64 ± 0.31 and 11.58 ± 0.39 kcal/mol for the 160, 400 and 600 ps simulations, respectively (Table 1). The 4′OH→4′CF_3 mutation is largely disfavored both in water and in ALR2. As for the 4′CH_3 mutation, the balance between free energies of 4′CF3 in the two different environments suggests that the gain in desolvation energy is offset by the formation of a less stable complex with ALR2. The

value of $\Delta\Delta G_{bind}$ obtained from the longer simulation is 1.49 kcal/mol (Table 2). Again, the 4′CF_3 derivative is predicted to be less active than the 4′OH reference compound. In the complex, 4′CF3 binds similarly to 4′CH3 [Fig. 2(b)]. Owing to the bulkier trifluoromethyl substituent, however, the inhibitor and Thr113 are further displaced as compared to 4′CH3, such that the distance between the substituent and the hydroxyl oxygen of Thr113 increases of about 0.3 Å. Compared to 4′-CH_3, the remarkable destabilization observed in the 4′CF3 free energy simulations partly arises from steric hindrance with Thr113, as indeed is the case of 4′-CH_3, and partly from even more non-complementary interactions with the oxygen of the Thr113 hydroxyl. In fact, the fluorine atoms have a partial negative charge and interaction with the hydroxyl oxygen is largely disfavoured. In this respect, we note that if the Thr113 hydroxyl is rotated of 180°, it turns to a hydrogen bond donor instead of an acceptor. This situation would partly alleviate unfavorable interactions with the trifluoromethyl substituent, which could accept a hydrogen bond from the hydroxyl. Even if the hydrogen bond acceptor capability of organic fluorine is questionable[23,24] and the free energy difference of solvation of CF_3 indicates that this substituent is hydrophobic, favorable electrostatic interactions between the negatively charged fluorine atoms and the hydroxyl hydrogen would, at least, help stabilizing the complex. To explore this possibility, the molecular dynamics trajectory of the longer simulation was examined, and showed that the Thr113 hydroxyl does not rotate of 180° during molecular dynamics. Rather, the hydroxyl firmly hydrogen bonds to the backbone carbonyl of Thr113 in the simulations [Fig. 2(b)]. Therefore, Thr113 can act solely as a hydrogen bond acceptor, and a hydrogen bond with trifluoromethyl cannot be formed.

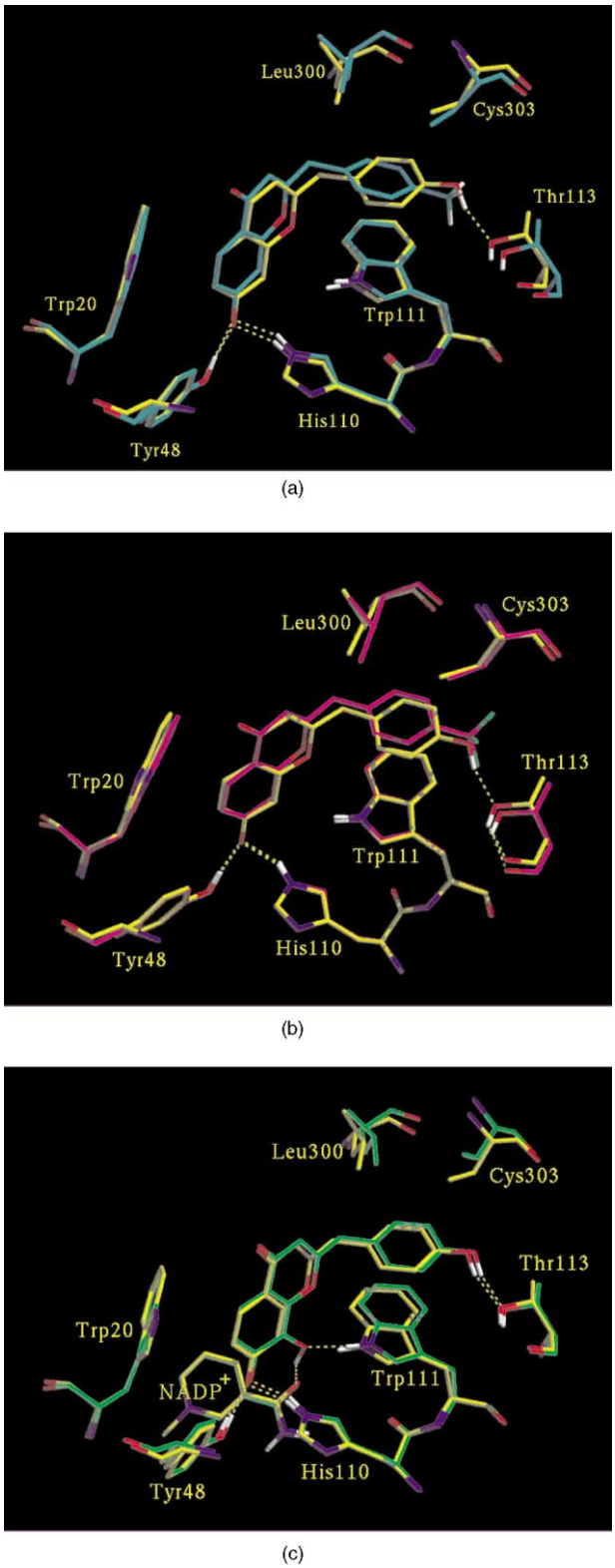

Figure 2. Selection of aminoacids that interact with 4′CH3 (a, cyan), 4′CF3 (b, magenta) and 8OH (c, green). The structure of 4′OH (yellow) is superimposed in each case, for comparison. Only polar hydrogens are shown, and water molecules are omitted.

Finally, the free energy changes upon mutating 8H into 8OH in ALR2 are -0.59 ± 0.02, -0.41 ± 0.11 and -0.65 ± 0.12 kcal/mol for the 160, 400 and 600 ps simulations, respectively (Table 1). While free energy differences are negative, that is the 8OH derivative is predicted to bind ALR2 more efficiently than the reference molecule, the net gain in free energy of binding to ALR2 is overcome by a higher desolvation cost. The value of $\Delta\Delta G_{bind}$ is 1.78 kcal/mol, leading to the prediction of a significant loss of binding. The 8-hydroxyl does, indeed, hydrogen bond to Trp111 and to the carbonyl oxygen of the nicotinamide, as initially predicted [Fig. 2(c)]. However, hydrogen bonds with these two residues are not as strong as with water, as free energies predict. In addition, some steric constraints between the 8-hydroxyl and the protein must be present in this case, since the 8-hydroxyl slightly displaces (of about 0.35 Å) the nearby Trp111 residue as compared to the reference compound [Fig. 2(c)].

Synthesis and biological evaluation

7-Hydroxy-2-(4′-trifluoromethylbenzyl)-4*H*-1-benzopyran-4-one **2** (4′-CF_3 in Scheme 1) was synthesized starting from 2-hydroxy-4-methoxy(methoxycarbonyl)acetophenone **2a** by reaction with 4-trifluoromethylphenyl acetylchloride in presence of $Mg(OEt)_2$ (Scheme 4) following a general procedure.[31] The methyl 7-methoxy-2-(4′-trifluoromethylbenzyl)-4*H*-

1-benzopyran-4-one-3-carboxylate **2b** thus obtained was saponified using HBr 48%, then decarboxylated by heating in quinoline. The subsequent treatment with BBr_3 allowed us to obtain the desired compound **2**.

7,8-Dihydroxy-2-(4′-hydroxybenzyl)-4*H*-1-benzopyran-4-one **3** (8-OH in Scheme 1) and 7-hydroxy-2-(4′-methylbenzyl)-4*H*-1-benzopyran-4-one **4** (4′-CH_3 in Scheme 1) were synthesized by the reaction between the appropriate 2-hydroxyacetophenone (**3a**, **4a**) and methyl 4-methoxyphenylacetate or methyl 4-methylphenylacetate respectively in presence of NaH/pyridine (Scheme 5); the intermediate 1,3-diketone was then cyclized to **3b** or **4** by treatment with hydrochloric acid/acetic acid; **3b** was then converted to **3** by treatment with BBr_3.

The inhibition constants (K_i) of the compounds were determined as described in the experimental part. The 4′CH_3, 4′CF_3 and 8OH derivatives proved to be less active than the reference 4′OH derivative, in agreement with predictions from FEP. The K_i values are reported in Table 2.

Discussion

In the present work, we have predicted the relative binding of three derivatives of 7-hydroxy-2-(4′-hydroxybenzyl)-4*H*-1-benzopyran-4-one to ALR2 by molecular dynamics and free energy perturbation calculations.

Conceptually, the relative binding of two related inhibitors to ALR2 ($\Delta\Delta G_{bind}$) can be analyzed as the sum of two components, the free energy difference of solvation of the ligands in water (ΔG_{solv}), and the free energy difference of binding to the protein (ΔG_{ALR2}). The difference between these two free energies ($\Delta\Delta G_{bind}$) determines the overall effectiveness of binding of the two related inhibitors. On interpretative grounds, while the ligand is fully solvated by water molecules before binding to the protein, water molecules are displaced (all or in part) and replaced with protein residues when the ligand approaches the binding site of the host. Therefore, a cost in free energy of solvation must be payed by the ligand to desolvate, and a gain in free energy of binding to the protein is obtained after formation of the complex. Figure 3 illustrates schematically the predictions of the relative free energies of binding that arise from the present study. In the fig. the black arrows (which correspond to $\Delta\Delta G_{bind}$) are the differences between the ΔG_{ALR2} and the ΔG_{solv} white arrows. A prediction of a less active inhibitor implies that the black arrow is directed toward the positive free energy axis, while, on the reverse, a more active inhibitor would have a black arrow toward the negative axis.

Substitution of the polar 4′OH with hydrophobic substituents like 4′CH_3 and 4′CF_3, which resulted in less solvated compounds, did not led to compounds that

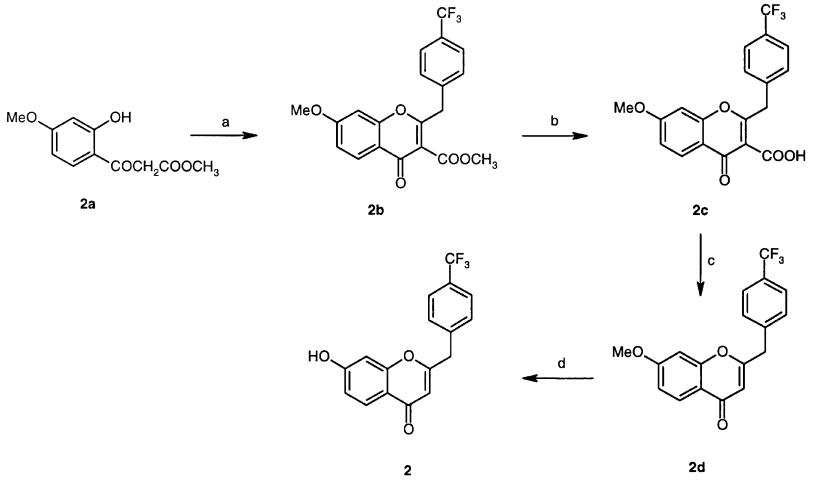

[a](a) $CF_3C_6H_4CH_2COCl$; $Mg(OEt)_2$; (b): HBr 48%; (c) Δ; (d): BBr_3.

Scheme 4. Synthetic route for 7-hydroxy-2-(4′-trifluoromethylbenzyl)-4*H*-1-benzopyran-4-one.

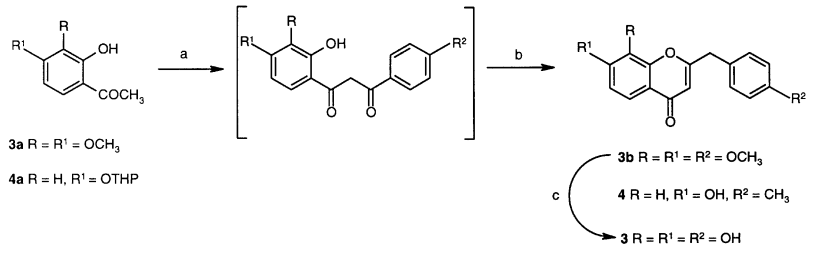

[a](a): $H_3COC_6H_4CH_2COOCH_3$ for **3b**, $H_3CC_6H_4CH_2COOCH_3$ for **4**, NaH; (b): CH_3COOH/HCl; (c): BBr_3.

Scheme 5. Synthetic route for 7-hydroxy-2-(4′-methylbenzyl)-4*H*-1-benzopyran-4-one and 7,8-dihydroxy-2-(4′-hydroxybenzyl)-4*H*-1-benzopyran-4-one.

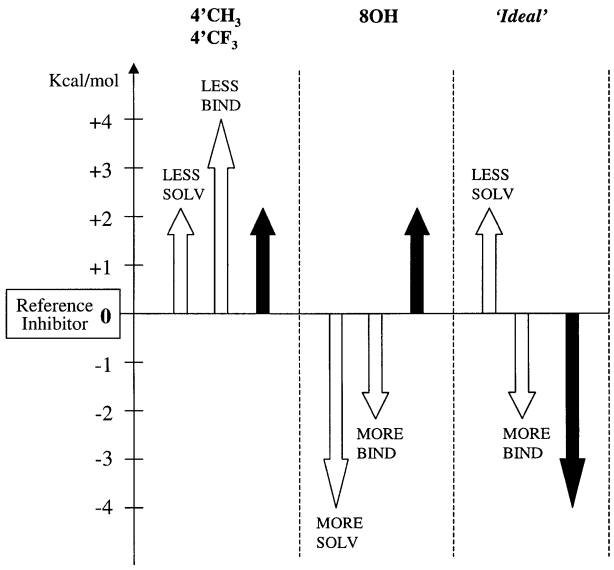

Figure 3. Schematic diagram showing the predictions of relative solvation and binding free energies that arise from the study. An '*ideal*' prediction is presented.

bind better to the enzyme (first case in Figure 3). While 4′CH_3 costs 5.72 kcal/mol less to desolvate as compared to 4′OH, it is predicted to bind ALR2 6.29 kcal/mol less favorably than 4′OH. Overall, since the loss of binding to ALR2 offsets the gain in desolvation, the 4′CH_3 is predicted to be less active than the 4′OH. The calculated value of $\Delta\Delta G_{bind}$ is 0.57 kcal/mol, which compares qualitatively with the experimental value of 1.12 inferred from the K_i's (Table 2). Similar reasonings hold for the 4′CF_3 derivative, which is 10.09 kcal/mol less solvated than the 4′OH, and 11.58 kcal/mol less apt to bind ALR2 than 4′OH. The predicted $\Delta\Delta G_{bind}$ of 1.49 kcal/mol for this compound is close to the experimental value of 1.67 kcal/mol (Table 2).

The results obtained for the 8OH derivative fall into the second case in Figure 3, where the perturbed ligand is both more solvated and more favourably bound to the enzyme. In this case, a desolvation penalty of −2.43 kcal/mol offsets a gain in binding of −0.65 kcal/mol, so that the 8OH derivative is predicted to be less active than 4′OH. The predicted $\Delta\Delta G_{bind}$ of 1.78 kcal/mol is in the ballpark of the experimental value of 2.42 kcal/mol as inferred from the K_i's (Table 2).

Finally, the third case in Fig. 3 can be regarded as the '*ideal*' condition for the prediction of a more active inhibitor, that is, the inhibitor is less solvated in water and better bound to the protein. In this case, the two factors sinergically enhance inhibition. This condition can be achieved, for example, by introducing suitable hydrophobic groups into the ligand, which decrease the desolvation penalty and enhance favorable interactions with hydrophobic residues. Unfortunately, none of the derivatives here presented fall into this case. While the substitution of the polar 4′OH with hydrophobic substituents resulted in less solvated compounds, they did not prove to bind better to the enzyme.

Experimental

Computational methods

The AMBER 5[32] program was used for all molecular mechanics (MM), molecular dynamics (MD) and free energy perturbation (FEP) calculations. The all-atom force field by Cornell et al.[25] was used. During MD and FEP simulations, all bond lenghts were constrained using the SHAKE[33] algorithm, allowing a time step of 2.0 fs. Solute and solvent were coupled to a constant temperature heat bath with a coupling constant of 0.2 ps to maintain a temperature of 300 K. A residue based cutoff of 10 Å was employed. Pairlists were updated every 10 time steps. In FEP, the entire inhibitor was treated as the perturbed group. No intraperturbed group contributions to the free energy were calculated.

The starting coordinates for FEP calculations were taken from our previous structure of the inhibitor 7-hydroxy-2-(4′-hydroxybenzyl)-4*H*-1-benzopyran-4-one bound in the active site of aldose reductase.[5] This structure was originally obtained starting from the coordinates of the human ALR2 holoenzyme[34] with inhibitors docked into the substrate binding site. The ternary complexes were energy-minimized and equilibrated using MD, as previously described.[5,10] This structure has the open additional hydrophobic pocket lined by Trp111 and Leu300 (whose relevance is discussed in refs 5, 8 and 10) and is very similar to the structure of aldose reductase that binds Zopolrestat, whose coordinates are still not completely available (only the backbone atoms and the inhibitor are present in the Protein Data Bank, entry code 1MAR[7]). In the structure of the protein, all Lys and Arg residues were positively charged, while Glu and Asp residues were negatively charged; the δH, εH or protonated forms of histidines were assigned on the basis of favorable interactions with their environment.

Counterions were placed around the charged residues at the surface of the enzyme-inhibitor complex in order to have a total charge of −1. The −1 charge was chosen so as to have the same net charge in the enzyme and in the water simulations (i.e., the negative charge of the dissociated 7-hydroxyl of the inhibitor). The oxidized form of NADPH ($NADP^+$) was used in all simulations because inhibitors preferentially bind this form.[35] The parameters for $NADP^+$ were taken from our previous simulations,[5] and those of fluorine were taken from the work of Gough et al.[30] As regards the inhibitors, their structures were completely optimized using AM1, and charges were calculated with electrostatic potential fits to a 6-31G* ab-initio wave function, followed by a RESP fit.[36,37] The partial atomic charges of the inhibitors are reported in Scheme 3.

Three independent perturbations were carried out starting from the reference inhibitor. In order to set up the perturbations, dummy atoms were added for the growing atoms (i.e., 4′OH→4′CH_3, 4′OH→4′CF_3, 8H→8OH). These dummy atoms had the same bonding parameters of the growing group, but zero charges and zero van der Waals parameters.

The active site of ALR2 containing the inhibitor and $NADP^+$ was solvated with a spherical cap of 1549 TIP3P[38] water molecules within 28 Å of the center of mass of the inhibitor, and harmonic radial forces (1.5 kcal/mol $Å^2$) were applied to these waters to avoid evaporation.

The energy minimization was performed by optimizing the water molecules first, keeping the rest of the system frozen. In addition, 20 ps MD at 300 K were performed on the water molecules only, in order to let the solvent equilibrate around the protein and the inhibitor. Then, energy minimization was continued by letting the inhibitor, $NADP^+$, all the protein residues within 12 Å from the inhibitor and all the water molecules free to move. 10,000 steps of conjugate grandient minimization were performed. Then, the minimized structure was equilibrated with MD at 300 K for 250 ps. During the first 10 ps of heating to 300 K, a 5 kcal/mol restraint was applied on the inhibitor and the protein residues, and then it was turned off.

The perturbations were carried out in a series of 40 windows with $\Delta\lambda = 0.025$. Simulations of increasing lenght were performed to test for convergence of the free energy results: 160ps (1000 steps of equilibration and 1000 steps of data collection at each window frame), 400 ps (2500 steps of equilibration and 2500 steps of data collection) and 600 ps (2500 steps of equilibration and 5000 steps of data collection). Simulations were run both in the forward ($\lambda = 1 \rightarrow 0$) and in the reverse ($\lambda = 0 \rightarrow 1$) direction, with 100 ps equilibration performed at $\lambda = 0$ before running the reverse simulation.

To obtain the structures of the $4'CH_3$, $4'CF_3$ and 8OH complexes, the end-point ($\lambda = 0$) of the longer (600 ps) ALR2-inhibitor perturbations were subjected to additional 100 ps MD, using the topology of the perturbed inhibitors. During these additional 100 ps, structures were collected every 0.2 ps and averaged every 10 ps, using CARNAL. Then, the last 10 ps-averaged structure was energy minimized with 10,000 steps of conjugate gradient minimization.

For mutations in water, the inhibitor was placed at the center of a rectangular box of 1250 TIP3P water molecules. The system was equilibrated at 300 K under periodic boundary conditions, using a minimization/equilibration simulation protocol similar to that above described. Then, mutations were performed as already described for aldose reductase.

Calculations were performed on an IBM-SP3 computer.

Chemistry

Melting points were determined on a Buchi 510 melting point apparatus and are uncorrected. ^{1}H NMR spectra were recorded on a Bruker AC200 spectrometer (Centro Interdipartimentale Grandi Strumenti, Modena University) in DMSO-d_6 solution. Chemical shifts are reported in ppm from tetramethylsilane as internal standard. J values are given in Hz. Microanalyses were carried out in the Microanalysis laboratory of the Dipartimento di Scienze Farmaceutiche, Modena University. Analyses indicated by the symbol of the elements were within $\pm 0.4\%$ of the theoretical values. TLC were performed on precoated silica gel F254 plates (Merck). Silica gel (Merck, 70–230 Mesh) was used for column chromatography.

The synthesis of 7-hydroxy-2-(4′-hydroxybenzyl)-4*H*-1-benzopyran-4-one **1** (4′OH in Scheme 1) is described in ref 5.

Methyl 7-methoxy-2-(4′-trifluoromethylbenzyl)-4*H*-1-benzopyran-4-one 3-carboxylate (2b). To a suspension of $Mg(OEt)_2$ (0.41 g, 3.58 mmol) in anhyd EtOH (10 mL) a solution of 2-hydroxy-4-methoxy(methoxycarbonyl)acetophenone **2a**[31] (0.81 g, 3.60 mmol) was added. A white precipitate formed. EtOH was then removed under reduced pressure, then anhyd benzene was added (30 mL) followed by 4-trifluoromethylphenylacetyl chloride (0.80 g, 3.60 mmol) dissolved in benzene (10 mL). The mixture was heated at reflux for 3 h, then it was cooled and poured in 10% acetic acid in water (100 mL) at 0 °C. The suspension was extracted with $CHCl_3$ (3 × 20 mL), the organic layer was dried (Na_2SO_4), the solvent removed under reduced pressure and the residue purified by column chromatography (cyclohexane/EtOAc 60:40). Yield 0.67 g (48%), mp 88–89 °C. ^{1}H NMR δ8.11 (1H, d, $J = 8.92$), 7.58 (4H, m), 7.12 (1H, dd, $J = 8.92$, $J = 2.38$), 6.77 (1H, d, $J = 2.35$), 4.14 (2H, s), 3.97 (3H, s), 3.90 (3H, s).

7-Methoxy-2-(4′-trifluoromethylbenzyl)-4*H*-1-benzopyran-4-one-3-carboxylic acid (2c). A suspension of **2b** (0.30 g, 0.77 mmol) in HBr 48% (15 mL) was heated at 110–120 °C for 14 h. After cooling, the precipitate was filtered and washed with water. Yield 0.20 g (69%), mp 179–80 °C. ^{1}H NMR δ 14.00 (1H, s), 8.02 (1H, m), 7.68 (4H, m), 7.13 (2H, m), 4.46 (2H, s), 3.91 (3H, s).

7-Methoxy-2-(4′-trifluoromethylbenzyl)-4*H*-1-benzopyran-4-one (2d). A solution of **2c** (0.10 g, 0.26 mmol) in quinoline (1.5 mL) was heated at 180 °C for 10 min, then cooled and poured in water (20 mL) containing concd. HCl (3 mL). The solid thus obtained was filtered and washed with water. Yield 0.070 g (80%), mp 182–185 °C. ^{1}H NMR δ 7.91 (1H, d, $J = 9.07$), 7.69 (4H, m), 7.04 (2H, m), 6.24 (1H, s), 4.15 (2H, s), 3.88 (3H, s).

7-Hydroxy-2-(4′-trifluoromethylbenzyl)-4*H*-1-benzopyran-4-one (2). To a solution of **2d** (0.070 g, 0.2 mmol) in anhyd CH_2Cl_2 (10 mL), under stirring at 0 °C, a solution of BBr_3 (1M in CH_2Cl_2, 1.05 mL, 1.05 mmol) in CH_2Cl_2 was added. The resulting solution was stirred at rt for 24 h, then cooled again; water was added and the precipitate was collected, washed with water and purified by means of preparative TLC (CH_2Cl_2/CH_3OH 97:3). Yield 0.005 g (7.5%), mp 162 °C (dec.) (diethyl ether/hexane). MS m/z 320 (M^+); ^{1}H NMR ($CDCl_3$) δ 8.07 (1H, d, $J = 8.73$), 7.52 (4H, m), 6.98 (1H, dd, $J = 8.76$, $J = 2.13$), 6.90 (1H, d, $J = 2.05$), 6.15 (1H, s), 3.99 (2H, s). Anal. ($C_{17}H_{11}F_3O_3$) C, H.

7,8-Dimethoxy-2-(4′-methoxybenzyl)-4*H*-1-benzopyran-4-one (3b). A solution of 2-hydroxy-3,4-dimethoxyacetophenone[39] **3a** (1.00 g, 5.1 mmol) and methyl 4-methoxyphenylacetate (1.00 g, 5.6 mmol) in anhyd pyridine (8 mL) was added dropwise to a well stirred suspension of NaH (60% dispersion in mineral oil) (0.72 g, 18.0 mmol) in anhyd pyridine (8 mL). When the reaction subsided, the mixture was heated at 90 °C for 15 min. After cooling, the mixture was decomposed in 2 N HCl and extracted with CH_2Cl_2 (3 × 25 mL). The combined organic layers were washed with 1N HCl (2 × 30 mL) and water (30 mL) and dried (Na_2SO_4); then the solvent was removed under reduced pressure. Yield 1.08 g (65%), mp 110–111 °C. ^{1}H NMR: 7.74 (1H, d, J = 8.97), 7.34 (2H, m), 7.22 (1H, d, J = 8.97), 6.94 (2H, m), 6.12 (1H, s), 3.97 (3H, s), 3.93 (2H, s), 3.77 (3H, s), 3.75 (3H, s).

7,8-Dihydroxy-2-(4′-hydroxybenzyl)-4*H*-1-benzopyran-4-one (3). To a stirred solution of **3b** (0.50 g, 1.53 mmol) in anhyd CH_2Cl_2 (30 mL) at 0 °C under N_2 atmosphere was added a BBr_3 solution in CH_2Cl_2 (1M, 9.20 mL, 9.20 mmol); the solution was left to stand at rt for 24 h, then it was cooled again to 0 °C, and water and ice were added. The resulting precipitate was collected and washed with water, then purified by column chromatography (CH_2Cl_2/CH_3OH 94:6). Yield 0.20 g (45%), mp 263–265 °C (CH_3OH/acetone). ^{1}H NMR δ 9.45 (3H, broad s), 7.34 (1H, d, J = 8.67), 7.20 (2H, m), 6.90 (1H, d, J = 8.67), 6.75 (2H, m), 5.96 (1H, s), 3.87 (2H, s). Anal. ($C_{16}H_{12}O_5$) C, H.

7-Hydroxy-2-(4′-methylbenzyl)-4*H*-1-benzopyran-4-one (4). A solution of 2-hydroxy-4-[2-(tetrahydropyranyl)-oxy]acetophenone[40] (1.0 g, 4.3 mmol) and methyl 4-methylphenyl acetate (0.77 g, 4.7 mmol) in anhyd pyridine (8 mL) was added dropwise to a well stirred suspension of NaH (60% dispersion in mineral oil) (0.52 g, 12.9 mmol) in anhyd pyridine (8 mL). When the reaction subsided, the mixture was heated at 90 °C for 15 min. After cooling, the mixture was decomposed in 2 N HCl and extracted with CH_2Cl_2 (3 × 25 mL). The combined organic layers were washed with 1N HCl (2 × 30 mL) and water (30 mL) and dried (Na_2SO_4); then the solvent was removed under reduced pressure. The residue was then purified by means of column chromatography (cyclohexane/EtOAc 75:25). Yield 0.95 g (84%), mp 178–181 °C (acetone/petroleum ether). ^{1}H NMR δ 10.69 (1H, s), 7.84 (1H, d, J = 8.67), 7.21 (4H, m), 6.88 (1H, dd, J = 8.69, J = 2.24), 6.78 (1H, d, J = 2.13), 6.01 (1H, s), 3.92 (2H, s), 2.29 (3H, s). Anal. ($C_{17}H_{14}O_3$) C, H.

Enzyme inhibition assays

Recombinant human aldose reductase was expressed as previously described.[41] Human recombinant aldose reductase were purified to electrophoretic homogeneity through the same chromatographic steps as previously described for the bovine enzyme.[42] The pure enzymes were stored at 4 °C in 10 mM sodium phosphate buffer pH 7.0 in the presence of 2 mM DTT.

Protein concentration was evaluated by the method of Bradford.[43] The electrophoretic homogeneity of enzyme preparations was assessed by SDS-PAGE according to the method of Laemmli[44] and gels were stained according to the method of Wray et al.[45]

The assay for aldose reductase activity was performed at 37 °C using 4.7 mM D,L-glyceraldehyde as substrate, in 0.25 M sodium phosphate buffer pH 6.8 containing 0.11 mM NADPH, 0.38 M ammonium sulfate and 0.5 mM EDTA. One Unit of enzyme activity is the amount of enzyme that catalyzes the oxidation of 1 μmol of NADPH/min.

The sensitivity of aldose reductase to different compounds was tested in the above assay conditions in the presence of the inhibitor dissolved at proper concentration in DMSO. The concentration of DMSO in the assay mixture was kept constant at 1%. For the determination of K_i double reciprocal plots with D,L-glyceraldehyde as variable substrate at fixed concentration of NADPH were obtained. For each inhibitor at least three different concentrations were used.

Elemental analyses

Compd	Formula	C Calcd/found	H Calcd/found
2	$C_{17}H_{11}F_3O_3$	63.76/63.41	3.46/3.48
3	$C_{16}H_{12}O_5$	67.60/67.91	4.25/4.20
4	$C_{17}H_{14}O_3$	76.68/76.89	5.30/5.18

Acknowledgements

Financial support from Consiglio Nazionale delle Ricerche (grant CNR 98.01911.CT03) is gratefully acknowledged.

References and Notes

1. Yabe-Nishimura, C. *Pharmacol. Rev.* **1998**, *50*, 21.
2. Costantino, L.; Rastelli, G.; Cignarella, G.; Vianello, P.; Barlocco, D. *Exp. Opin. Ther. Pat* **1997**, *7*, 843.
3. Costantino, L.; Rastelli, G.; Vianello, P.; Cignarella, G.; Barlocco, D. *Med. Res. Rev.* **1999**, *19*, 3.
4. Eggler, J. F., Larson, E. R., Lipinski, C. A., Mylari, B. L., Urban, F. J. In *A Perspective of Aldose Reductase Inhibitors. Advances In Medical Chemistry*. Jai: Greenwich, CT, 1993; Vol. 2, p. 197.
5. Costantino, L.; Rastelli, G.; Gamberini, M. C.; Vinson, J. A.; Bose, P.; Iannone, A.; Staffieri, M.; Antolini, L.; Del Corso, A.; Mura, U.; Albasini, A. *J. Med. Chem.* **1999**, *42*, 1881.
6. Costantino, L.; Rastelli, G.; Albasini, A. *Eur. J. Med. Chem.* **1996**, *31*, 693.
7. Wilson, D. K.; Tarle, I.; Petrash, J. M.; Quiocho, F. A. *Proc. Natl. Acad. Sci. U.S.A.* **1993**, *90*, 9847.
8. Urzhumtsev, A.; Tete-Favier, F.; Mitscler, A.; Barbanton, J.; Barth, P.; Urzhumgtseva, L.; Biellmann, J. F.; Podjarny, A. D.; Moras, D. *Structure* **1997**, *5*, 601.

9. Costantino, L.; Rastelli, G.; Vescovini, K.; Cignarella, G.; Vianello, P.; Del Corso, A.; Cappiello, M.; Mura, U.; Barlocco, D. *J. Med. Chem.* **1996**, *39*, 4396.
10. Rastelli, G.; Vianello, P.; Barlocco, D.; Costantino, L.; Del Corso, A.; Mura, U. *Bioorg. Med. Chem. Lett.* **1997**, *7*, 1897.
11. Rastelli, G.; Costantino, L. *Bioorg. Med. Chem. Lett.* **1998**, *8*, 641.
12. Rastelli, G.; Costantino, L.; Vianello, P.; Barlocco, D. *Tetrahedron* **1998**, *54*, 9415.
13. Bohren, K. M.; Grimshaw, C. E.; Lai, C. J.; Harrison, D. H.; Ringe, D.; Petsko, G. A.; Gabbay, K. H. *Biochemistry* **1994**, *33*, 2021.
14. Grimshaw, C. E.; Bohren, K. M.; Lai, C. J.; Gabbay, K. H. *Biochemistry* **1995**, *34*, 14374.
15. Kollman, P. A. *Chem. Rev.* **1993**, *93*, 2395.
16. Fox, T.; Scanlan, T. S.; Kollman, P. A. *J. Am. Chem. Soc.* **1997**, *119*, 11571.
17. McCarrick, M. A.; Kollman, P. A. *J. Comp-Aided Drug Des* **1999**, *13*, 109.
18. Reddy, M. R.; Erion, M. D. *J. Am. Chem. Soc.* **2001**, *123*, 6246.
19. Pearlman, D. A.; Charifson, P. S. *J. Med. Chem.* **2001**, *44*, 3417.
20. Bash, P. A.; Singh, U.; Langridge, R.; Kollman, P. A. *Science* **1987**, *236*, 564.
21. McCammon, J. A. *Science* **1987**, *238*, 486.
22. Jorgensen, W. L.; Briggs, J. M. *J. Am. Chem. Soc.* **1989**, *111*, 4190.
23. Dunitz, J. D.; Taylor, R. *Chem. Eur. J.* **1997**, *3*, 89.
24. Howard, J. A. K.; Hoy, V. J.; O'Hagan, D.; Smith, G. T. *Tetrahedron* **1996**, *52*, 12613.
25. Cornell, W. D.; Cieplak, P.; Bayly, C. I.; Gould, I. R.; Merz, K. M., Jr.; Ferguson, D. M.; Spellmeyer, D. C.; Fox, T.; Caldwell, J. W.; Kollman, P. A. *J. Am. Chem. Soc.* **1995**, *117*, 5179.
26. Kollman, P. A. *Accounts Chem. Res.* **1996**, *29*, 461.
27. Wang, J.; Cieplak, P.; Kollman, P. A. *J. Comput. Chem.* **2000**, *21*, 1049.
28. Wang, W.; Donini, O.; Reyes, C. M.; Kollman, P. A. *Annu. Rev. Biophys. Biomol. Struct.* **2001**, *30*, 211.
29. Cheatham, T. E., III.; Kollman, P. A. *Annu. Rev. Phys. Chem.* **2000**, *51*, 435.
30. Gough, C. A.; DeBolt, S. E.; Kollman, P. A. *J. Comput. Chem.* **1992**, *13*, 963.
31. Cushman, M.; Nagarathnam, D.; Burg, D. L.; Gealen, R. L. J. *Med. Chem.* **1991**, *34*, 798.
32. Case, D. A.; Pearlman, D. A.; Caldwell, J. W.; Cheatman, T. E., III.; Ross, W. S.; Simmerling, C. L.; Darden, T. A.; Merz, K. M.; Stanton, R. V.; Cheng, A. L.; Vincent, J. J.; Crowley, M.; Ferguson, D. M.; Radmer, R. J.; Seibel, G. L.; Singh, U. C.; Weiner, P. K.; Kollman, P. A. *AMBER 5*; University of California: San Francisco, 1997.
33. van Gunsteren, W. F.; Berendsen, H. J. C. *Mol. Phys.* **1977**, *34*, 1311.
34. Wilson, D. K.; Bohren, K. M.; Gabbay, K. H.; Quiocho, F. A. *Science* **1992**, *257*, 81.
35. Ehrig, T.; Bohren, K. M.; Prendergast, F. G.; Gabbay, K. H. *Biochemistry* **1994**, *33*, 7157.
36. Bayly, C. I.; Cieplak, P.; Cornell, W. D.; Kollman, P. A. *J. Phys. Chem.* **1993**, *97*, 10269.
37. Cieplak, P.; Bayly, C. I.; Cornell, W. D.; Kollman, P. A. *J. Comput. Chem.* **1995**, *16*, 1357.
38. Jorgensen, W. L.; Chandrasekhar, J.; Madura, J. D.; Impey, R. W.; Klein, M. L. *J. Chem. Phys* **1983**, *79*, 926.
39. Baker, W. *J. Chem. Soc* **1941**, 662.
40. Sogawa, S.; Nihro, Y.; Ueda, H.; Miki, T.; Matsumoto, H.; Satoh, T. *Biol. Pharm. Bull.* **1994**, *17*, 251.
41. Petrash, J. M.; Harter, T. M.; Devine, C. S.; Olins, P. O.; Bhatnagar, A.; Liu, S.; Srivastava, S. K. *J. Biol. Chem.* **1992**, *267*, 24833.
42. Del Corso, A.; Barsacchi, D.; Giannessi, M.; Tozzi, M. G.; Camici, M.; Mura, U. *Arch. Biochem. Biophys.* **1990**, *283*, 512.
43. Bradford, M. M. *Anal. Biochem.* **1976**, *72*, 248.
44. Laemmli, U. K. *Nature* **1970**, *227*, 680.
45. Wray, W.; Boulikas, T.; Wray, W. P.; Hancock, R. *Anal. Biochem.* **1981**, *118*, 197.